The emergence of spiraling tracheary element bundles in incompatible grafts

Huiyan Wu [1], **Zhuying Deng** [1], **Xue Wang** [1], **Dacheng Liang** [Corresp. 1]

[1] School of Agriculture, Yangtze University, Jingzhou, Hubei, 434023, China; Engineering Research Center of Ecology and Agricultural Use of Wetland, Ministry of Education, Yangtze University, Jingzhou, Hubei Province, China

Corresponding Author: Dacheng Liang
Email address: dachengliang@gmail.com

In distantly related plant grafting, incompatibility often occurs between scion and rootstock, resulting in growth stagnation, and eventually graft failure. In this study, we found that an emergent structure, or the spiraling tracheary element (TE) bundles consisting of TE masses occurring at the graft interface, was extensively present in the highly incompatible interfamilial graft of *Brassica napus/Portulaca oleracea* (*Bn/Po*) and *Nicotiana benthamiana/Portulaca oleracea* (*Nb/Po*). This special structure mostly appeared in the local area near the grafting union, and the frequency and quantity of the spiraling tracheary element bundles were much higher in the scion than in the rootstock. Nevertheless, only a small portion of *Arabidopsis thaliana/Portulaca oleracea* (*At/Po*) interfamilial grafts showed a less spiraled TEs at the grafting union (usually a circular TE), which is consistent with its growth performance. This study consolidated that spiraling TE bundles were an important indicator for graft incompatibility. The possible reason for the formation of spiraling TE bundles in interfamilial grafts was discussed.

1   # The Emergence of Spiraling Tracheary Element Bundles in

2   # Incompatible Grafts

4   Huiyan Wu, Zhuying Deng, Xue Wang and Dacheng Liang[*]

6   *School of Agriculture, Yangtze University, Jingzhou, Hubei, 434023, China; Engineering*

7   *Research Center of Ecology and Agricultural Use of Wetland, Ministry of Education, Yangtze*

8   *University, Jingzhou, Hubei, 434023, China*

10   Corresponding Author:

11   Dacheng Liang

12   No. 266, Jingzhou City, Hubei Province, 434023, China

13   Email address: dachengliang@gmail.com

14

15   **Abstract**

16   In distantly related plant grafting, incompatibility often occurs between scion and rootstock, resulting in growth

17   stagnation, and eventually graft failure. In this study, we found that an emergent structure, or the spiraling tracheary

18   element (TE) bundles consisting of TE masses occurring at the graft interface, was extensively present in the highly

19   incompatible interfamilial graft of *Brassica napus/Portulaca oleracea* (*Bn/Po*) and *Nicotiana*

20   *benthamiana/Portulaca oleracea* (*Nb/Po*). This special structure mostly appeared in the local area near the grafting

21   union, and the frequency and quantity of the spiraling tracheary element bundles were much higher in the scion than

22   in the rootstock. Nevertheless, only a small portion of *Arabidopsis thaliana/Portulaca oleracea* (*At/Po*) interfamilial

23   grafts showed a less spiraled TEs at the grafting union (usually a circular TE), which is consistent with its growth

24   performance. This study consolidated that spiraling TE bundles were an important indicator for graft

25   incompatibility. The possible reason for the formation of spiraling TE bundles in interfamilial grafts was discussed.

26

27   **Introduction**

28   Grafting is one of the artificial propagation methods of plants, in which two different plant segments are

29   mechanically joined together to survive as a new individual after vascular connection and wound healing. This

30   technique was practiced in ancient Greece and China as early as the 5th century BC (Melnyk & Meyerowitz 2015).

31   At present, it is widely used in agricultural production and horticultural research.

32   The compatibility between scion and rootstock is the key factor affecting the grafting success. A prerequisite

33   for successful grafting and long-term survival is the taxonomic closeness of the scion to the stock. In general,

34 different species of plants in the same genus can form effective union and survive, while grafting of plants in

35 different genera of the same family are rarely compatible (Goldschmidt 2014). In some special cases, grafting

36 between distant species, such as *Arabidopsis* and tomato, despite the lack of vascular connection, the *Arabidopsis*

37 scion grafted onto tomato rootstock can still blossom and produce seeds (Flaishman et al. 2008). However, due to

38 the low efficiency of nutrition and hormone transfer between tissues, it is still doubtful whether these grafts can be

39 maintained for a long time (Melnyk 2017). So far, the mechanism of the incompatibility of heterograft is still

40 unclear, and practical graft work relies largely on empirical observation for horticultural production.

41   The connection of vascular bundle after grafting is one of the important signs of grafting success (Melnyk

42 2017; Melnyk & Meyerowitz 2015). The cuts introduced during grafting necessitate the destruction of the vascular

43 system of plants, resulting in the discontinuity of vascular transport of water, nutrients and various organic materials

44 (Asahina & Satoh 2015). Therefore, the connection of the vascular system between graft partners needs to be

45 quickly re-established for survival. However, various factors including the taxonomic relatedness, anatomical

46 structure (e.g. the necrotic layer at the graft interface), mechanical mismatch during grafting, pathological infections,

47 growth condition and growth activity of either graft partner could cause the graft failure (Hartmann et al. 2011).

48 Mosse (1962) proposed that destruction of vascular continuity due to abnormalities of vascular development at the

49 graft union caused graft incompatibility. In a recent study, formation of a spiraling tracheary element bundle

50 (spiraling TE bundle) in the graft union was strongly associated with graft incompatibility in the

51 *Arabidopsis*/*Nicotiana* interfamilial graft (Deng et al. 2021). This further suggests that vascular behavior was critical

52 for graft union formation.

53   To further test whether this particular vascular structure was occurring in other interfamilial grafts, we focused

54 on interfamilial combination involving purslane as rootstock. The existence of spiraling TEs in the interfamilial

55 grafts, i.e. the *Brassica napus*/*Portulaca oleracea* (*Bn/Po*), *Nicotiana benthamiana*/*Portulaca oleracea* (*Nb/Po*) and

56 *Arabidopsis thaliana*/*Portulaca oleracea* (*At/Po*) combination was described, and the causes of their formation and

57 their influence on the growth of distant grafting were also discussed.

58

59 Materials and methods

60 Experimental materials

61   The seeds of rape (*Brassica napus*), *Nicotiana benthamiana*, *Arabidopsis thaliana* and purslane (*Portulaca*

62 *oleracea*) were surface-sterilized in chlorine gas for 2 hours. Then they were plated on the sterile MS medium

63 containing 3% sucrose (W/V). Sterile petri dishes containing seeds were vertically placed in the growth room for

64 constant temperature growth (22 ~ 23℃), and the growth condition was set at long-day photoperiod cycle (16 h of

65 light and 8 h of darkness).

66 Micrografting

67   Seedlings germinated after 7-9 days on MS medium were selected for grafting (purslane as rootstock, rape,

68 *Nicotiana benthamiana* and *Arabidopsis* as scion respectively). The grafting process was described previously

69 (Deng et al. 2021). Grafts were grown on moisturized Whatman paper for 3 days, then gently moved to MS medium

70 containing 3% sucrose (w/v) with forceps and continued to grow in a growth room (16 h light /8 h darkness) at 22-

71 23 ℃.

Vasculature isolation, Scanning Electron Microscopy and Counting of the Spiraling TE Bundles

74 Isolation of vasculature was recently described by Liu et al. (2022) and Deng et al. (2021). The leaves and roots
75 of grafts were removed and soaked in 0.04% saponin solution for 30min, then washed with PEM solution (50 mM
76 PIPES, 5 mM EGTA, 2.5 mM MgSO4, pH 6.9) for 3 times, and then fixed in 4% paraformaldehyde in PEM buffer
77 for 30min. The fixed samples were washed with PEM solution and then dissected to remove the tissues adjacent to
78 the vascular bundles under a dissecting microscope. The longitudinally dissected vascular samples were treated with
79 the enzyme cocktail solution consisting of 5 mM 2-(N-morpholino) ethanesulfonic acid (MES), 0.5％ (w/v)
80 cellulase (Sigma, EC 3.2.1.4), 0.2% (v/v) pectinase (Sigma, EC 3.2.1.15), 0.12 M sucrose, 1 mM $CaCl_2$ (pH 5.5) at
81 28 ℃ for 1.5 h. The treated samples were washed in 5% TritonX-100 for 15 minutes and then in PEM solution for
82 15 minutes. Samples were dehydrated step by step (15 min each) with 15%, 30%, 50%, 75% and 100% alcohol.
83 With another two times of absolute ethanol wash, they were dried for 3 h in a −20 ℃, low-vacuum drier (CHRIST).
84 The dried samples were mounted on the sample holder, and then placed in the ion sputtering apparatus (SC7620
85 Sputter coater) for conductive gold coating. Examination of the samples was conducted in a VEGA3 TESCAN
86 scanning electron microscope at 20 kv acceleration voltage. In order to count for the number of spiraling bundles,
87 we surveyed the area within a 3 mm radius centered at the midpoint of the grafting interface. The spiraling bundle
88 was characterized with spiraling tracheary elements plus either a concave hole or convex point, and thus was
89 counted as a spiraling bundle. The *Arabidopsis*/purslane grafts (n = 67) were surveyed every two days after grafting,
90 while rape/purslane grafts (n = 35) and *Nicotiana*/purslane grafts (n = 43) were mainly surveyed after 28 DAG. For
91 each time of collection, graft unions from at least six individual grafts were prepared.

Results

Three interfamilial grafts using purslane as rootstock

94 In this experiment, we constructed three interfamilial grafts, the *Bn*/*Po* heterograft (Fig. 1A, B), *At*/*Po* heterograft
95 (Fig. 1D, E), and *Nb*/*Po* heterograft (Fig. 1H, I), and four self-grafts, i.e. the *Bn* (Fig. 1C), *At* (Fig. 1F), *Po* (Fig. 1G)
96 and *Nb* (Fig. 1J) self-graft by micrografting technique. Nearly all the *Bn*/*Po* grafts remained quiescent (Fig. 1A), a
97 growth status similar to some grafts of *At*/*Nb* combination described previously (Deng et al. 2021), suggesting the
98 two species were highly incompatible. The *At*/*Po* grafts, however, grew very quickly in the 20 days after grafting,
99 suggesting that *Arabidopsis* and purslane was potentially compatible with each other at this stage (Fig. 1D). Usually,
100 a delayed incompatibility was observed around 30 days after grafting; either the grafts ceased growth, or the grafts
101 developed adventitious roots at the graft union (Table 1). The *Nb*/*Po* grafts displayed yellowing of foliage (Fig. 1H,
102 Table 1), suggesting poor development of scion shoot. In addition, the graft unions in both *Bn*/*Po* and *Nb*/*Po* grafts
103 were enlarged (Fig. 1B, I), implying a structural expansion within the unions. In the compatible self-grafts of *Bn*, *At*,
104 *Po* and *Nb*, the growth of each species was normal (Fig. 1C, F, G and J).

Emergence of spiraling TE bundles or circular TE at the graft union

106 The scion and the rootstock of the *Bn*/*Po* heterografts were easily parted during the preparation for SEM,

107   implying fragile connection between scion and rootstock. The SEM examination showed that spiraling TE bundles

108   extensively existed at the graft union of *Bn*/*Po* combination (Fig. 2A), and around 80% of grafts produced spiraling

109   TE bundles at the graft union (Fig. 2B). These spiraling bundles were mainly confined to the upper part of grafting

110   interface, and they strongly rejected the connection with TEs from rootstock. A single circular tracheary element

111   could also be formed through self-fusion as shown in Fig. 2A (shown in red circle), and a repeated process of

112   circling led to the formation of spiraling bundles (Fig. 2A). Apparently, these spiraling bundles lost their TE end,

113   and did not provide a tapered or inclined end wall for overlapping or fusion as normal TE did, therefore could not

114   make a connection with the TEs from rootstock.

115   In *At*/*Po* grafts, the frequency of spiraling TE bundle formation was relatively low (Fig. 2C, D), and about

116   16.7% of grafts (10 out of 60) harbored circular TEs (Fig. 2E). Moreover, the TEs were loosely spiraled (Fig. 2C),

117   thus they usually existed as a single ring and rarely formed a highly spiraling structure (Fig. 2C, D). In fact, the

118   *At*/*Po* grafts grew well in the first 20 days, agreeing with the less-forming spiraling bundles.

119   We further examined the spiraling TEs in the scion of *Nicotiana benthamiana* belonging to solanaceae family,

120   diverging more than 100 million years ago from brassicaceae family according to Ku et al. (2000). Similarly, the

121   enlarged union was consisted of more spiraling TEs (Fig. 2F) which were either convolute concave (Fig. 2G) or

122   convex (Fig. 2H). In an extreme case, these small spirals were fused to form chignon-like structure (Fig. 2I). More

123   than 65% of these grafts contained various numbers of spirals, of whom the majority were two spirals (Fig. 2J). In

124   all compatible self-grafts, there was no spiraling TE bundle detected (Table 1). Taken together, the more compatible

125   *At*/*Po* combination has less spiraling TEs than in *Bn*/*Po* and *Nb*/*Po* combination (Fig. 2K, Table 1), suggesting a

126   close association of graft incompatibility with emergence of spiraling TEs.

127

Discussion

129   In our recent study, we found that the spiraling TE bundles existed in almost all the quiescent grafts of

130   *Arabidopsis/Nicotiana* combination, but they appeared rarely in the grafts with active growth (Deng et al. 2021).

131   These bundles were most likely built on circular vessels (Deng et al. 2021). The circular vessels were observed in

132   injury-induced wood tumor of *Picea excelsa* (Lam.) Lk (Włoch 1976). Similarly, the circular vessels were also

133   formed close to transverse wounds, e.g. the wounds at the inflorescence stems of *Arabidopsis* (Mazur et al. 2016), at

134   the basal side of the radish root and in basal swellings above the cut surfaces of pea stems about a week after the

135   plant was cut (Sachs 1981; Sachs & Cohen 1982). They were also formed at branch junctions of various tree species

136   (Lev-Yadun & Aloni 1990; Rothwell & Lev-Yadun 2005), in the suppressed or dormant buds that were oriented

137   across the trunk of *Ficus religiosa* (Aloni & Wolf 1984). Usually, these circular structures occurred relatively rare

138   and irregularly in different parts of the plant. The spiraling TE bundles reported here and also by Deng et al. (2021)

139   were widespread at the grafting interface of incompatible grafts. We also observed the occurrence of chignon-like

140   sphere structure consisting of small spirals at the *Nb*/*Po* interface (Fig. 2I), which looked like the previously

141   described vascular nodules found in the bud grafting apple tree (Mosse & Labern 1960). These evidence suggested

142   the formation of the circular vessels might play an important part in grafting process.

143   Sachs (1984) proposed that the differentiation of circular vessels was related to the circulating flux of auxin.

144   When auxin accumulated near the grafting union, the polarity of signal transmission would be reversed locally with

145   diffusion, resulting in the formation of circular vessels in local areas above the grafting interface. Nevertheless, this

146   explanation might only partially account for the spiraling bundle formation as transverse wounds or injuries usually

147   led to small circular vessels as mentioned above. We did not observe the occurrence of spiraling bundles in the

148   compatible self-grafts of purslane (Table 1), *Arabidopsis* or *Nicotiana* (Table 1; Deng et al., 2021), or of quinoa (Liu

149   et al. 2022). The repeated formation of circular vessel at the grafting interface indicated that the spiraling structure

150   could result from the distant scion-rootstock interaction, or alternatively, simply from the emergent property of

151   perturbed auxin flux by heterografting, or both. In addition, it's easy to comprehend that the spiraling TE bundles

152   could also occur, though in a low frequency, at the rootstock region below the grafting interface where auxin

153   accumulation was much less due to scion-rootstock disconnection.

154

155   **Conclusions**

156   Spiraling TE bundles were widespread existed in incompatible grafts. They restricted the graft growth and

157   potentially blocked the vascular connection, thus could be used an important indicator of incompatibility of distant

158   grafts. In practice, we can use this structure to examine the possible grafting relationship between scion and

159   rootstock. Furthermore, future study could be designed to address the origin and molecular mechanisms of spiraling

160   TE bundles.

161

162   **Author contributions**

163   Huiyan Wu: material construction, collection, SEM examination, discussion and writing of the manuscript.

164   Zhuying Deng: material construction and sample collection.

165   Xue Wang: regents and materials preparation.

166   Dacheng Liang: study conception, SEM analysis, discussion and writing of the manuscript.

167   **Acknowledgments**

168   We would like to thank Dr. Rosemary White for her helpful discussions on this work.

169   **Disclosure of interest**

170   No potential conflict of interest was reported by the authors.

171   **Funding**

172   No funding for this work was received.

173   **Data Availability Statement**

174   The authors confirm that the data supporting the findings of this study are available within the article.

175   **References**

176   Aloni R, and Wolf A. 1984. Suppressed Buds Embedded in the Bark Across the Bole and the Occurrence of their
177   Circular Vessels in Ficus religiosa. *American Journal of Botany* 71:1060-1066. 10.2307/2443381
178   Asahina M, and Satoh S. 2015. Molecular and physiological mechanisms regulating tissue reunion in incised plant
179   tissues. *J Plant Res* 128:381-388. 10.1007/s10265-015-0705-z
180   Deng Z, Wu H, Jin T, Cai T, Jiang M, Wang M, and Liang D. 2021. A Sequential Three-Phase Pathway Constitutes

181   Tracheary Element Connection in the Arabidopsis/Nicotiana Interfamilial Grafts. *Frontiers in plant science*
182   12. 10.3389/fpls.2021.664342

183   Flaishman MA, Loginovsky K, Golobowich S, and Lev-Yadun S. 2008. *Arabidopsis thaliana* as a model system for
184   graft union development in homografts and heterografts. *Journal of Plant Growth Regulation* 27:231-239.

185   Goldschmidt EE. 2014. Plant grafting: new mechanisms, evolutionary implications. *Frontiers in plant science* 5.
186   10.3389/fpls.2014.00727

187   Hartmann HT, Kester DE, Davies FT, and Geneve RL. 2011. *Hartmann and Kester's Plant Propagation: Principles*
188   *and Practices*. New York: Pearson; 8th edition.

189   Ku H-M, Vision T, Liu J, and Tanksley SD. 2000. Comparing sequenced segments of the tomato and *Arabidopsis*
190   genomes: Large-scale duplication followed by selective gene loss creates a network of synteny. *Proceedings*
191   *of the National Academy of Sciences* 97:9121-9126. doi:10.1073/pnas.160271297

192   Lev-Yadun S, and Aloni R. 1990. Vascular differentiation in branch junctions of trees: circular patterns and functional
193   significance. *Trees* 4:49-54. 10.1007/BF00226240

194   Liu X, Wu H, Zeng Y, Deng Z, Wang X, and Liang D. 2022. The dynamic changes of tracheary elements in an
195   intraspecific quinoa (*Chenopodium quinoa*) graft. *J Plant Physiol*:153691. 10.1016/j.jplph.2022.153691

196   Mazur E, Benková E, and Friml J. 2016. Vascular cambium regeneration and vessel formation in wounded
197   inflorescence stems of Arabidopsis. *Scientific Reports* 6:33754. 10.1038/srep33754

198   Melnyk CW. 2017. Plant grafting: insights into tissue regeneration. *Regeneration* 4:3-14. 10.1002/reg2.71

199   Melnyk CW, and Meyerowitz EM. 2015. Plant grafting. *Current Biology* 25:R183-188. 10.1016/j.cub.2015.01.029

200   Mosse B. 1962. *Graft-incompatibility in fruit trees : with particular reference to its underlying causes*. Farnham
201   Royal, Bucks: Commonwealth Agricultural Bureaux.

202   Mosse B, and Labern MV. 1960. The Structure and Development of Vascular Nodules in Apple Bud-unions. *Annals*
203   *of botany* 24:500-507.

204   Rothwell GW, and Lev-Yadun S. 2005. Evidence of polar auxin flow in 375 million-year-old fossil wood. *Am J Bot*
205   92:903-906. 10.3732/ajb.92.6.903

206   Sachs T. 1981. The Control of the Patterned Differentiation of Vascular Tissues. In: Woolhouse HW, ed. *Advances in*
207   *Botanical Research*: Academic Press, 151-262.

208   Sachs T. 1984. Axiality and polarity in vascular plants. In: Barlow PW, and Carr DJ, eds. *Positional controls in plant*
209   *development*. Cambridge, UK: Cambridge University Press, 193-224.

210   Sachs T, and Cohen D. 1982. Circular Vessels and the Control of Vascular Differentiation in Plants. *Differentiation*
211   21:22-26. 10.1111/j.1432-0436.1982.tb01189.x

212   Włoch W. 1976. Cell events in cambium, connected with the formation and existence of a whirled cell arrangement.
213   *Acta Societatis Botanicorum Poloniae* 45:313.

214

Figure 1

Heterografts of *Bn*/*Po*, *At*/*Po* and *Nb*/*Po* combination and self-grafts of *Bn*, *At*, *Po* and *Nb* species.

(A) The representative plants of *Bn*/*Po* heterografts showing growth stagnation. (B) The graft union of the *Bn*/*Po* heterograft. (C) *Bn* self-graft. (D) A representative plant of *At*/*Po* heterograft. (E) The graft union of the *At*/*Po* heterograft. (F) *At* self-graft. (G) *Po* self-graft. (H) A representative plant of *Nb*/*Po* heterograft. (I) The graft union of the *Nb*/*Po* heterograft. (J) *Nb* self-graft. Arrow indicates the graft union.

Figure 2

Occurrence of spiraling TE bundles in interfamilial graft.

(A) A typical *Bn/Po* graft interface showing the widespread formation of spiraling TE bundles in the scion of *Bn/Po* graft at 28 DAG. The red circle indicates a single circular TE of rape. (B) Occurrence of various spirals in *Bn/Po* grafts. Data (mean ± SD) were generated in three repeats (n = 9, 12, and 14 respectively). (C) A small circular TE occurring in the scion of *At/Po* graft at 15 DAG. (D) A small circular TE (the red circle) occurring in the rootstock of *At/Po* graft at 27 DAG. (E) Occurrence of various spirals in *At/Po* grafts. Data (mean ± SD) were generated in three repeats (n = 20, 22, and 25 respectively). (F) The widespread formation of spiraling TE bundles in the scion of *Nb/Po* graft at 28 DAG. (G) The concave spiral. (H) The convex spiral. (I) The fused spirals were formed into chignon-like sphere structure. (J) Occurrence of various spirals in *Nb/Po* grafts. Data (mean ± SD) were generated in three repeats (n = 10, 13, and 20 respectively). (K) Occurrence percentage (mean ± SD) of spiraling TEs between *At/Po*, *Nb/Po* and *Bn/Po* grafts. Student's *T*-test was used to generate the *p*-value. *, ** indicated $p < 0.05$ and $p < 0.01$ respectively.
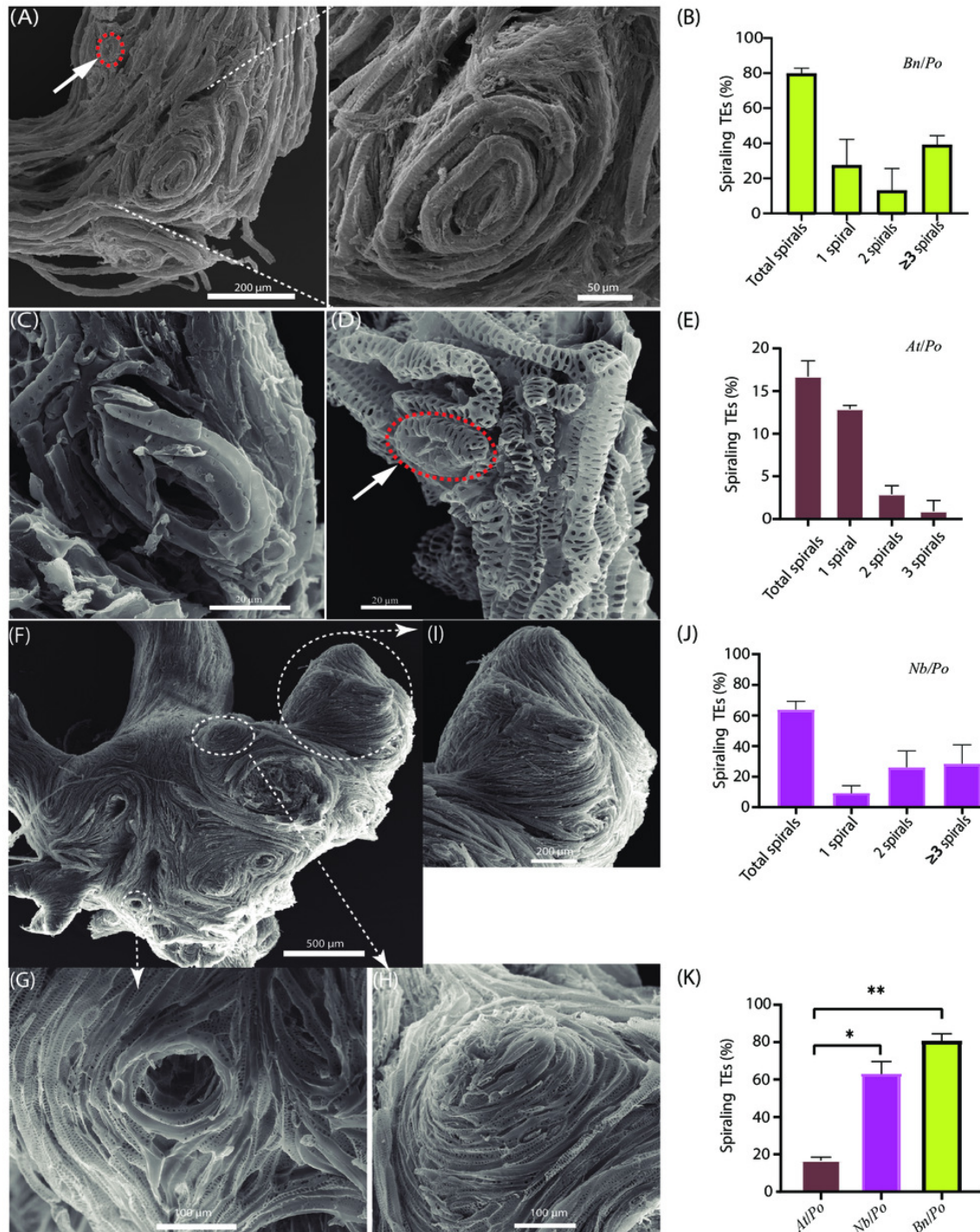
Graft compatibility and occurrence of spiraling bundles.

2   Table 1. Graft compatibility and occurrence of spiraling bundles.

Grafts	Graft union	Adventitious roots	Retarded growth	Yellowing of foliage	Occurrence of Spiraling bundles	Graft Compatibility
Bn/Po	enlarged	17.1%	82.9%	51.4%	80%	incompatible
At/Po	smooth	58.7%	17.4%	54.3%	16.3%	Partially incompatible
Nb/Po	enlarged	60.7%	16.6%	100%	64.2%	Highly incompatible
At/At	smooth	1%	0	0	0	Fully compatible
Po/Po	smooth	0	0	0	0	Fully compatible
Nb/Nb	smooth	0	0	0	0	Fully compatible